AD-A154 577 FORM FACTOR EFFECTS ON MICROWAVE CERENKOV RADIATION(U) 1/1
NAVAL POSTGRADUATE SCHOOL MONTEREY CA E R TURNER
DEC 84

UNCLASSIFIED F/G 20/8 NL

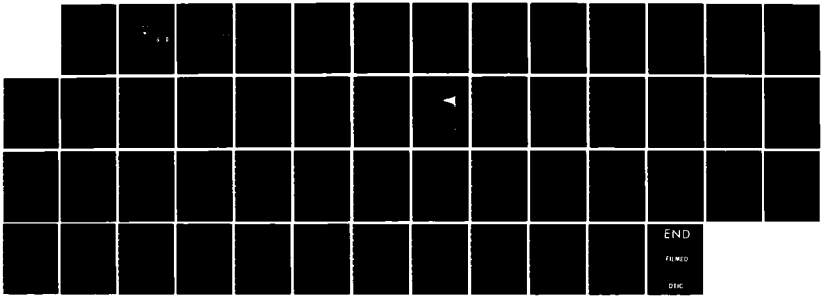

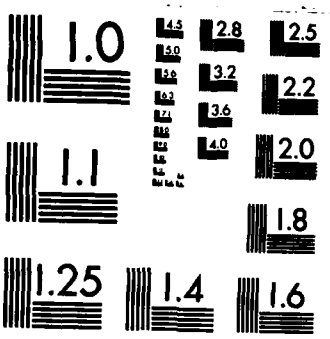

NAVAL POSTGRADUATE SCHOOL
Monterey, California

THESIS

FORM FACTOR EFFECTS ON MICROWAVE CERENKOV RADIATION

by

Edward R. Turner

December 1984

Thesis Advisor: John R. Neighbours

Approved for public release; distribution is unlimited.

Unclassified

SECURITY CLASSIFICATION OF THIS PAGE (When Data Entered)

REPORT DOCUMENTATION PAGE		READ INSTRUCTIONS BEFORE COMPLETING FORM
1. REPORT NUMBER	2. GOVT ACCESSION NO.	3. RECIPIENT'S CATALOG NUMBER
4. TITLE (and Subtitle) Form Factor Effects on Microwave Cerenkov Radiation		5. TYPE OF REPORT & PERIOD COVERED Master's Thesis December 1984 6. PERFORMING ORG. REPORT NUMBER
7. AUTHOR(s) Turner, Edward R.		8. CONTRACT OR GRANT NUMBER(s)
9. PERFORMING ORGANIZATION NAME AND ADDRESS Naval Postgraduate School Monterey, CA 93943		10. PROGRAM ELEMENT, PROJECT, TASK AREA & WORK UNIT NUMBERS
11. CONTROLLING OFFICE NAME AND ADDRESS Naval Postgraduate School Monterey, CA 93943		12. REPORT DATE December 1984 13. NUMBER OF PAGES 50
14. MONITORING AGENCY NAME & ADDRESS(if different from Controlling Office)		15. SECURITY CLASS. (of this report) Unclassified 15a. DECLASSIFICATION/DOWNGRADING SCHEDULE
16. DISTRIBUTION STATEMENT (of this Report) Approved for public release; distribution unlimited		
17. DISTRIBUTION STATEMENT (of the abstract entered in Block 20, if different from Report)		
18. SUPPLEMENTARY NOTES (20		
19. KEY WORDS (Continue on reverse side if necessary and identify by block number) Microwave Cerenkov Radiation; Stimulated Cerenkov Radiation		

Accession For
NTIS GRA&I
DTIC TAB
Unannounced
Justification
By
Distribution/
Availability Codes
Dist | Avail and/or Special
A/1

20. ABSTRACT (Continue on reverse side if necessary and identify by block number)

The effects of the electron bunch charge distribution on the production of microwave Cerenkov radiation in air are investigated. The representation of this distribution is presented in terms of a function called the form factor. Theory is developed which uses two dimensionless quantities to study the form factor effects. These are the emission length to wavelength ratio and the bunch length to wavelength ratio. A

DD FORM 1 JAN 73 1473 EDITION OF 1 NOV 65 IS OBSOLETE
S/N 0102-LF-014-6601

Unclassified

SECURITY CLASSIFICATION OF THIS PAGE (When Data Entered)

prediction is made for conditions which allows a concentration of radiation ninety degrees to the beam. Results are reported of experiments which were performed to measure the effects of the form factor using parameters available at the Naval Postgraduate School's linear accelerator. Findings from these experiments along with suggestions for further research are included.

Keywords include:

19

Approved for public release; distribution is unlimited.

Form Factor Effects on Microwave Cerenkov Radiation

by

Edward R. Turner
Lieutenant Commander, United States Navy
B.S., University of New Mexico, 1976

Submitted in partial fulfillment of the
requirements for the degree of

MASTER OF SCIENCE IN PHYSICS

from the

NAVAL POSTGRADUATE SCHOOL
December 1984

Author: Edward R. Turner
Edward R. Turner

Approved by: John R Neighbours
John R. Neighbours, Thesis Advisor

Xavier K. Maruyama
Xavier K. Maruyama, Co-Advisor

G E Schacher
G. E. Schacher, Chairman,
Department of Physics

J M Dyer
J. M. Dyer,
Dean of Science and Engineering

ABSTRACT

The effects of the electron bunch charge distribution on the production of microwave Cerenkov radiation in air are investigated. The representation of this distribution is presented in terms of a function called the form factor. Theory is developed which uses two dimensionless quantities to study the form factor effects. These are the emission length to wavelength ratio and the bunch length to wavelength ratio. A prediction is made for conditions which allows a concentration of radiation ninety degrees to the beam. Results are reported of experiments which were performed to measure the effects of the form factor using parameters available at the Naval Postgraduate School's linear accelerator. Findings from these experiments along with suggestions for further research are included.

TABLE OF CONTENTS

LIST OF TABLES

LIST OF FIGURES

ACKNOWLEGEMENTS

I wish to thank my thesis advisors, Professors J. R. Neighbours and X. K. Maruyama, and Professor F. R. Buskirk for the instruction, guidance and assistance they provided. I am especially grateful to Mr. Don Snyder for his continuous support and technical expertise that guided me through the experiments.

Finally, I wish to thank my wife, Kathleen, for her love and understanding throughout this effort.

I. INTRODUCTION

A. BACKGROUND

A charged particle (electron) which travels through a medium at a speed greater than the (phase) velocity of light in the same medium will generate a continuous spectrum of electromagnetic radiation. This process is referred to as Cerenkov radiation. The nature of Cerenkov radiation differs quite dramatically from that which is produced by other means. Most notable is its highly pronounced asymmetry: the radiation is emitted at an angle acute to the direction of motion of the electron. This phenomenon is closely analogous to the acoustic shock wave, produced by a supersonic projectile, which is emitted in a cone whose vertex is on the line of motion of the source. For Cerenkov radiation, the direction of this cone is defined by the Cerenkov angle.

$$\cos\theta_c = c/v \tag{1.1}$$

where c is the speed of light in the medium and v is the velocity of the electron. The Cerenkov angle is measured with respect to the direction of motion of the electron. To illustrate this idea, Figure 1.1 describes geometrically how a point charge traveling at a velocity v, where v is greater than the velocity of light c, will produce a wavefront at time t=5. The Cerenkov angle is then determined by constructing a perpendicular to the resultant wavefront. The angle of the intersection of this perpendicular with the direction of the source is the Cerenkov angle.

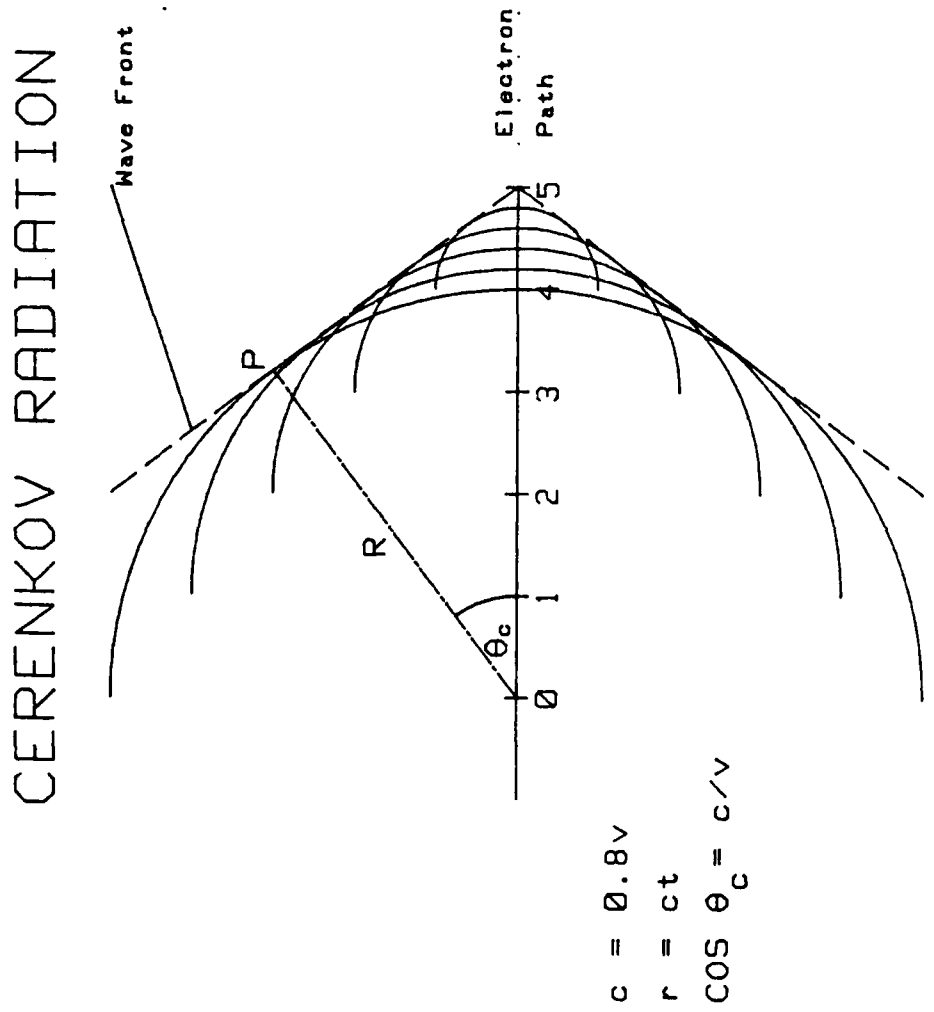

Figure 1.1 Cerenkov Radiation

The distribution of intensity of incoherent Cerenkov radiation is proportional to the frequency throughout the range in which the index of refraction is greater than one. Thus, the intensity at microwave frequencies would normally be negligible unless the electron beam was periodically bunched so as to radiate coherently. This concept is the topic of the investigations performed by J.R. Neighbours and F.R. Buskirk in [Ref. 1] and [Ref. 2].

B. DISCUSSION OF THEORY

Neighbours and Buskirk developed the equations for the power from Cerenkov microwave radiation emitted by a traveling wave electron accelerator (LINAC) in [Ref. 2]. The fact that the length over which the electrons are able to emit radiation is finite results in the radiation propagation direction no longer being confined to the sharp Cerenkov angle, θ_C, but spread over a range of emission angles. The expression for the power radiated per unit solid angle can be written as

$$W(\nu,n)=(\mu/2c)[L\nu\nu_o \sin\theta\rho(k)I(u)]^2 \qquad (1.2)$$

The parameters used to describe the radiation are

$$u=(kL/2)(c/v-\cos\theta) \qquad (1.3)$$

$$I(u)=\sin(u)/u \qquad (1.4)$$

$$\rho(\vec{k}) \cdot \int d^3r\ e^{-i\vec{k}\cdot\vec{r}}\rho(\vec{r}) \qquad (1.5)$$

where $\vec{k}$ is in the emission direction, ν is the frequency of the emitted radiation, L is the emission path length. $\rho(\vec{r})$ is the charge density distribution for a single electron bunch and ν_o is the LINAC operating frequency, which is equal to the electron bunch velocity, v, divided by the electron bunch spacing.

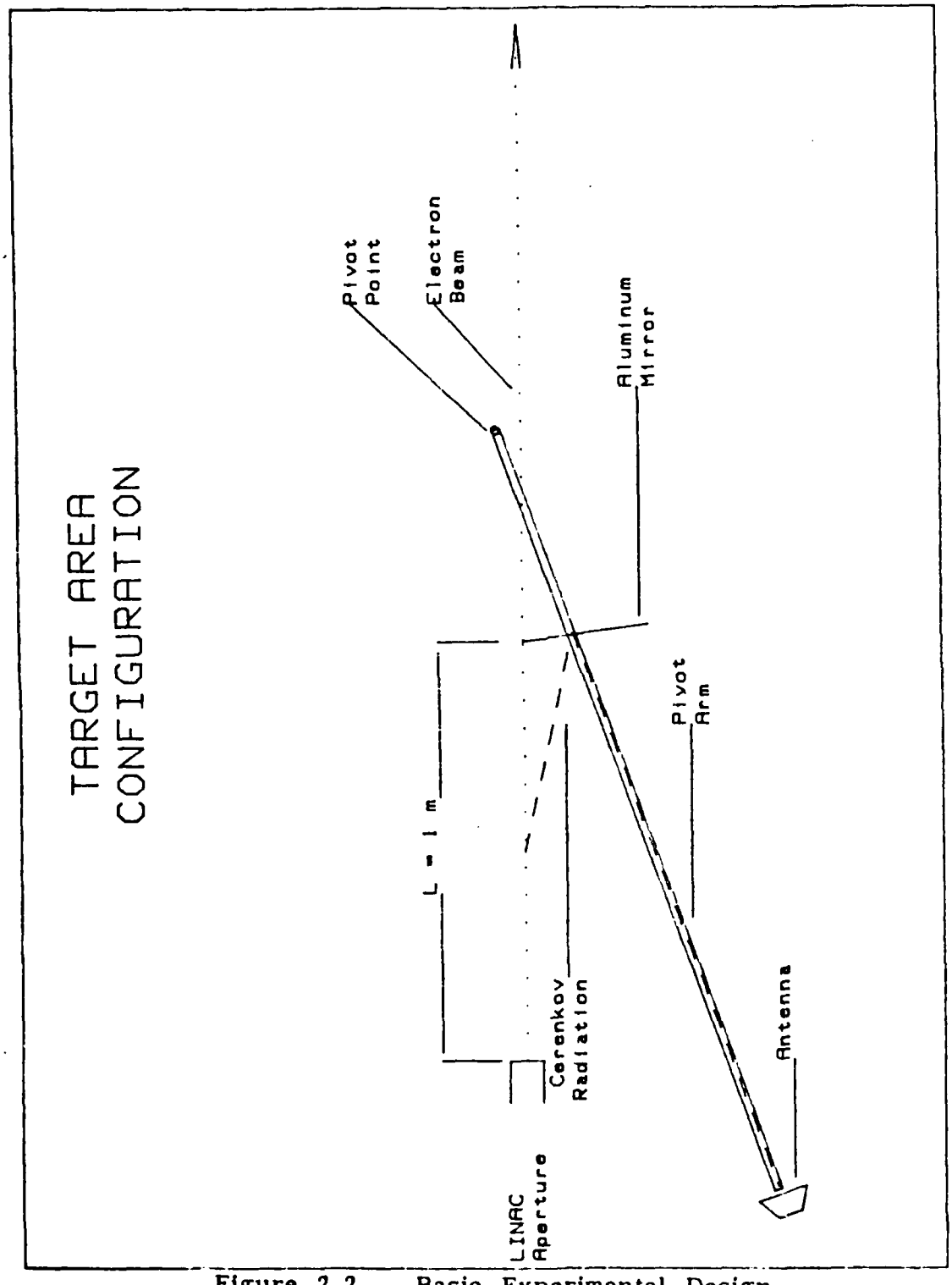

Figure 2.2 Basic Experimental Design

An emission length, L, of one meter was used by Newton [Ref. 4] and Saglam in [Ref. 6]. This length is the practical limit due to the physical restrictions of the LINAC target area. One meter was shown to provide adequate signal strength for processing within the X band frequency range (8.2 to 12.4 GHz).

Consideration was also given for a shorter emission length. Using general antenna theory, it was estimated that an emission region on the order of 15 centimeters would enable the detector to be placed in the far field region. The loss of signal strength for this length would require some method of amplification.

The basic experimental configuration was similar to that used by Newton, and described in [Ref. 4], The general arrangement of equipment in the target area is shown in Figure 2.2. The electrons exit the linac through an aperture and pass by an aluminum mirror. A portion of the Cerenkov microwave radiation produced by the electrons during the period travelled between the aperture and the mirror will be reflected by the mirror and travel to the detector.

There were two methods considered for the detection of the Cerenkov microwave radiation. Each method has certain advantages and certain limitations.

The first method used a Tektronix 7L18 Spectrum Analyzer. This spectrum analyzer is capable of detecting signals whose frequencies lie between 1 and 18 GHz. By using available external mixers, the frequency range can be extended to include frequencies up to 60 GHz. This method of detection is similar to that used by Pugh which is described in [Ref. 5]. The difficulties he encountered with ambiguities at higher frequencies when using the Tektronix 491 Spectrum Analyzer were expected to be at least partially eliminated with the improvements incorporated in the 7L18.

The ability of the spectrum analyzer to detect frequencies up to the twenty-first harmonic made this method of detection very attractive. Comparing figure 2.3 to figure 2.4 provides an indication that as frequency increases, the difference in signal strength

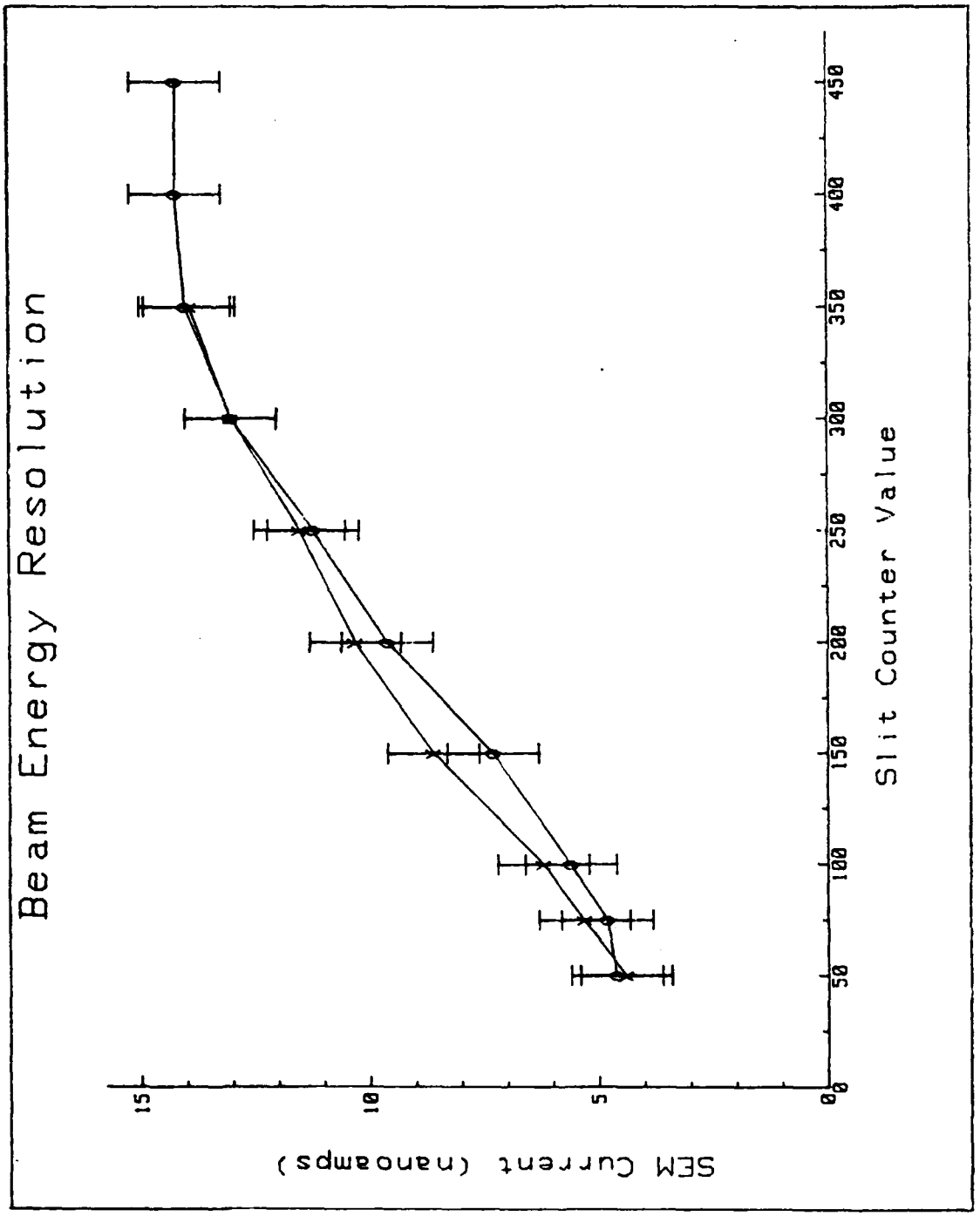

Figure 2.1 Electron Beam Current versus Slit Opening

where the term $\Delta E/E$ represents the energy resolution of the LINAC.

This energy resolution is determined by an energy defining slit whose size can be adjusted at the LINAC control station. The size of the slit is monitored by an installed digital counter. The relation between this counter value and the actual slit size was provided by a calibration curve developed in August, 1971. The curve displayed a linearity which can be described by

$$SS=2.24\times10^{-5}CV-9.47\times10^{-5} \qquad (2.2)$$

where SS is the slit size expressed in meters and CV is the digital counter value. Additional information obtained at the LINAC facility indicates that a slit size of .584 centimeters corresponds to an energy resolution of one percent, and a slit size of .318 centimeters corresponds to a resolution of .5 percent. Assuming a linear relation between slit size and energy resolution and using equation 2.2,

$$\Delta E/E=4.20\times10^{-5}CV-1.13\times10^{-3} \qquad (2.3)$$

To determine the limits on b, an preliminary set of data was taken for the electron beam current as a function of slit size. This data is presented in figure 2.1. The data reveals a linearity between the beam current and the size of the slit opening up to a counter value of about 350 (.775 cm), at which point, no increase in current is observed. Using equation 2.3, this upper limit would correspond to a resolution of 1.36 percent. The narrowest slit opening was dictated by operational considerations and corresponded to a counter value of 50. This meant that the most monoenergetic beam obtainable had a resolution of .097 percent. Using equation 2.1, these limiting values produce available electron bunch lengths ranging from .276 to .074 centimeters.

II. EXPERIMENT

A. BASIC DESIGN

The purpose of this experiment was to measure the effects of the electron bunch size on the emitted Cerenkov radiation. In order to accomplish this, it was first necessary to consider the limitations imposed by the various components involved in producing, detecting, and measuring the microwave radiation. The limiting cases could then be considered in the experimental design.

The Naval Postgraduate School's LINAC was used to provide the high energy electrons necessary to produce Cerenkov radiation. The specifications for this LINAC are provided in table 1.

TABLE 1
NPS Linac Specifications

Electron Energy	100 MeV
Maximum Average Current	0.3 microamps
Operating Frequency	2.856 GHz
Pulse Repetition Rate	60 pps
Pulse Duration	1 microsecond

The electron beam current is measured by means of a secondary emission monitor (SEM) which has a stated efficiency of six percent. Thus, a measured SEM value of 15 nanoamps would equate to a beam current of 0.25 microamps.

The temporal structure of the electron bunches is related to the LINAC energy resolution. This relation is explained in [Ref. 1] and is included in Appendix A. The resulting equation for the bunch length parameter b, is

$$b=v(2\pi\nu_{\bullet})^{-1}[2\Delta E/E]^{1/2} \qquad (2.1)$$

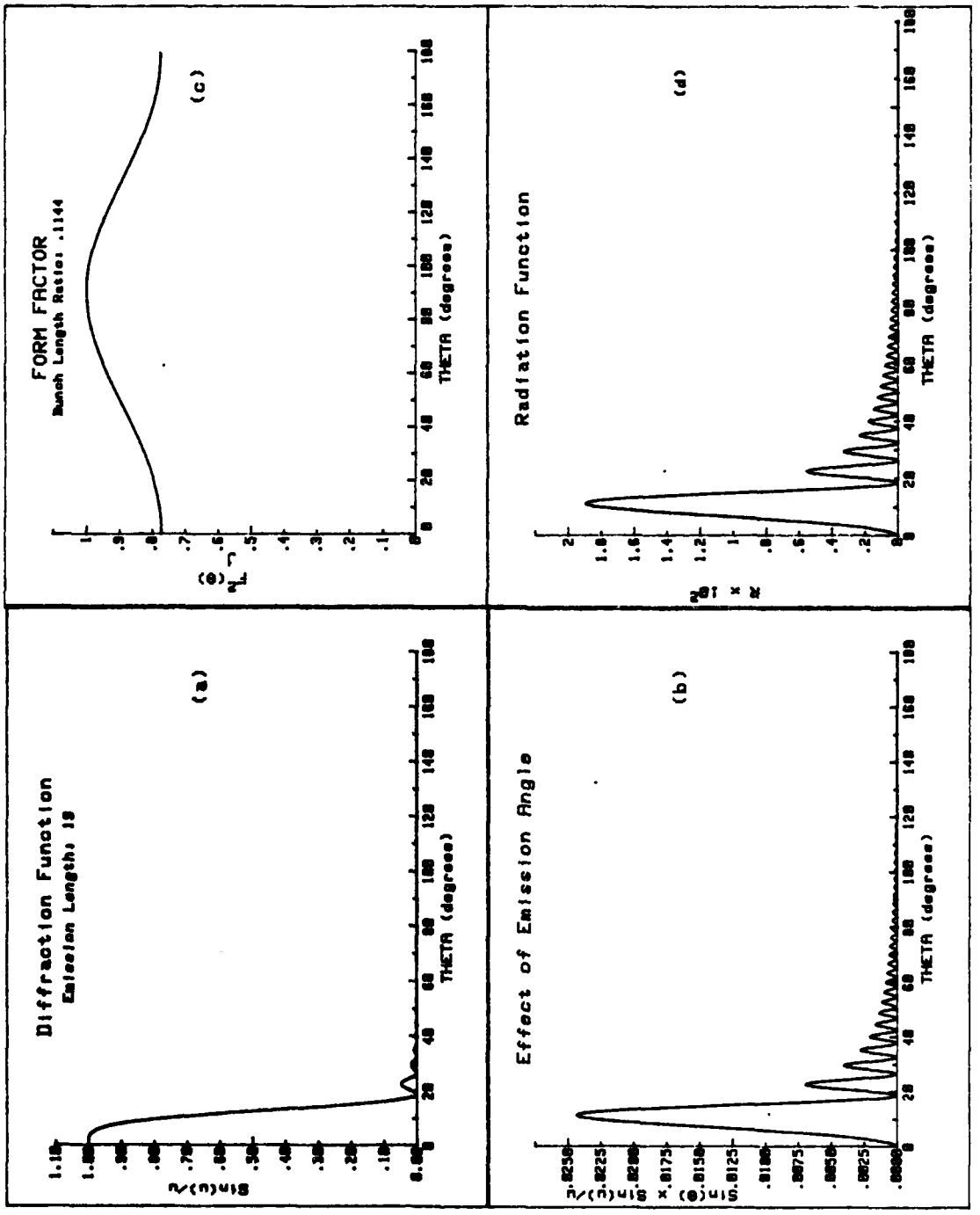

Figure 1.5 Radiation Produced by Second Harmonic

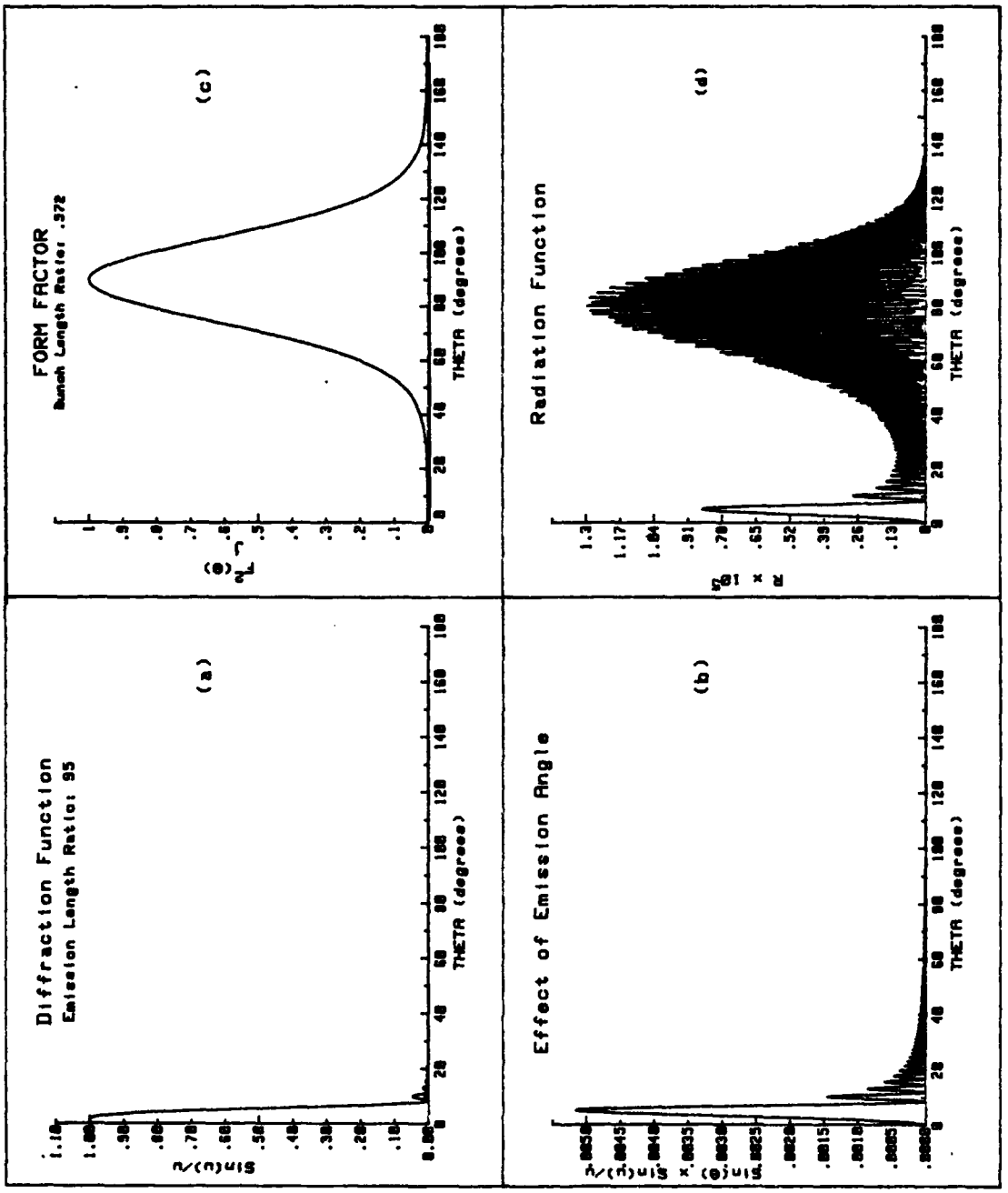

Figure 1.4 Production of Cerenkov Radiation Normal to the Electron Beam

example, the maximum observable peak power form the second harmonic is about sixty times greater than for the tenth harmonic.

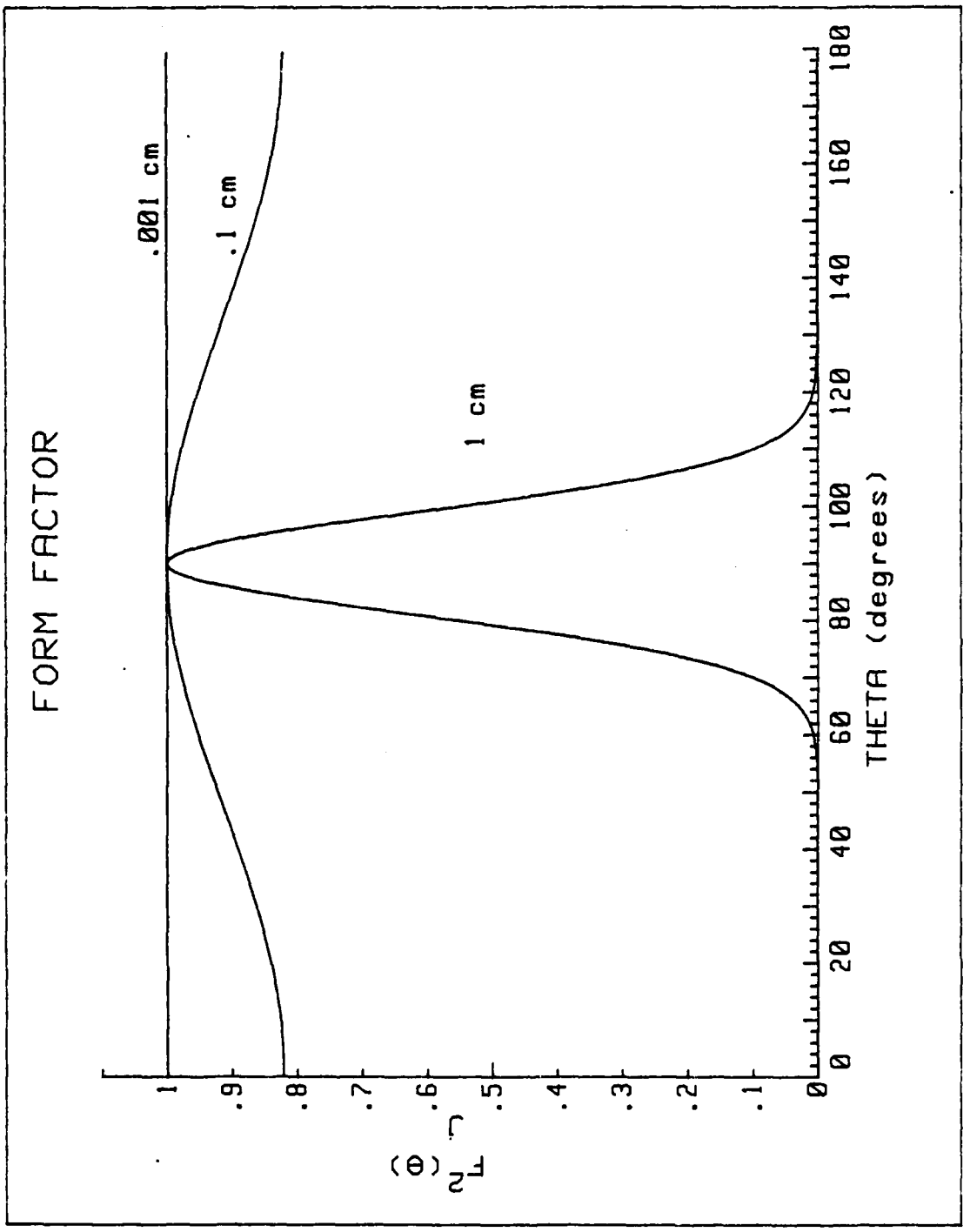

Figure 1.3 Effects of the Bunch Length Ratio

The effects of the emission length ratio and the bunch length ratio on the Cerenkov power radiated can be readily observed by looking at the expression for the normalized radiation function,

$$R \equiv D_j(\theta)/(\nu_o^2 j^2 L^2) = \sin^2\theta I^2(u) F^2(k) \qquad (1.18)$$

Observe that, for large values of the bunch length ratio, the form factor will contribute significantly to the reduction of the main lobe generated by the diffraction function. If, at the same time, the emission length ratio is small, a condition could be achieved where the majority of the Cerenkov power is radiated in a direction normal to the electron beam path.

Figure 1.4 demonstrates graphically how the various components of equation 1.18 contribute to the resulting power distribution. For this illustration, an emission length ratio of 95 and a bunch length ratio of 0.572 were chosen. These would be the resulting values for the tenth harmonic of a 2.85 GHz LINAC with an emission length of one meter and a gaussian bunch length of 1.2 centimeters (b=0.6 cm). Figure 1.4(a) shows the diffraction function, I(u), as a function of emission angle. As expected, this function tends to direct most of the radiation along the beam path. The product of the diffraction function and $\sin^2\theta$ is presented in Figure 1.4(b). Note that the forward peak is moved away from the beam path and its magnitude is substantially reduced. Finally, when this function is combined with the form factor in Figure 1.4(c), the resulting distribution presented in Figure 1.4(d) shows the forward lobe again reduced so much so that the radiation occuring at ninety degrees is actually larger. This value of the radiation function is about 1.3×10^{-5}. As a comparison, Figure 1.5 develops the same sequence as described above for the second harmonic. The same emission length and bunch length parameter is used. In this case, the form factor has much less of an effect on the forward peak, and the majority of the radiation is directed forward. The value of the radiation function for this peak is about 1.9×10^{-2}. For this

radiation can occur, that being equal to c, then equation 1.14 indicates a minimum emission length of $\lambda/2$. Simply stated, the radiation emitted by the electron just as it enters the emission region and the radiation emitted by the same electron as it leaves the emission region will exactly cancel each other at a point normal to the center of this region.

We can now focus our attention on the form factor. If we assume the charge distribution is gaussian as assumed in [Ref. 1], then

$$F(k)=\exp[-k_x^2a^2/4-k_y^2a^2/4-k_z^2b^2/4] \qquad (1.15)$$

For a LINAC whose electrons radiate in air with a Cerenkov angle of several degrees, k_xa and k_ya in equation 1.15 can be neglected since the perpendicular extent of the beam is much smaller than the beam extent along its path. In that case,

$$F(k)=\exp[-k_z^2b^2/4] \qquad (1.16)$$

which can be rewritten in terms of the radiation wavelength as

$$F(k)=\exp[-\pi^2(b/\lambda)^2\cos^2\theta] \qquad (1.17)$$

where k_z has been replaced by $k\cos\theta$.

The behavior of the form factor over the range of emission angles is dependent on the ratio of the electron bunch length parameter to the wavelength of the emitted radiation. If this ratio is very small, ($b<<\lambda$), the value of F is essentially unity for all angles and can be taken as independent of the emission angle. However, if larger values of this bunch length ratio are considered, the value of F over the range of emission angles can take on values significantly less than one. In this case, the form factor's dependence on the angle is very dramatic since at ninety degrees, the cosine term goes to zero causing a form factor of unity. Figure 1.3 illustrates this effect.

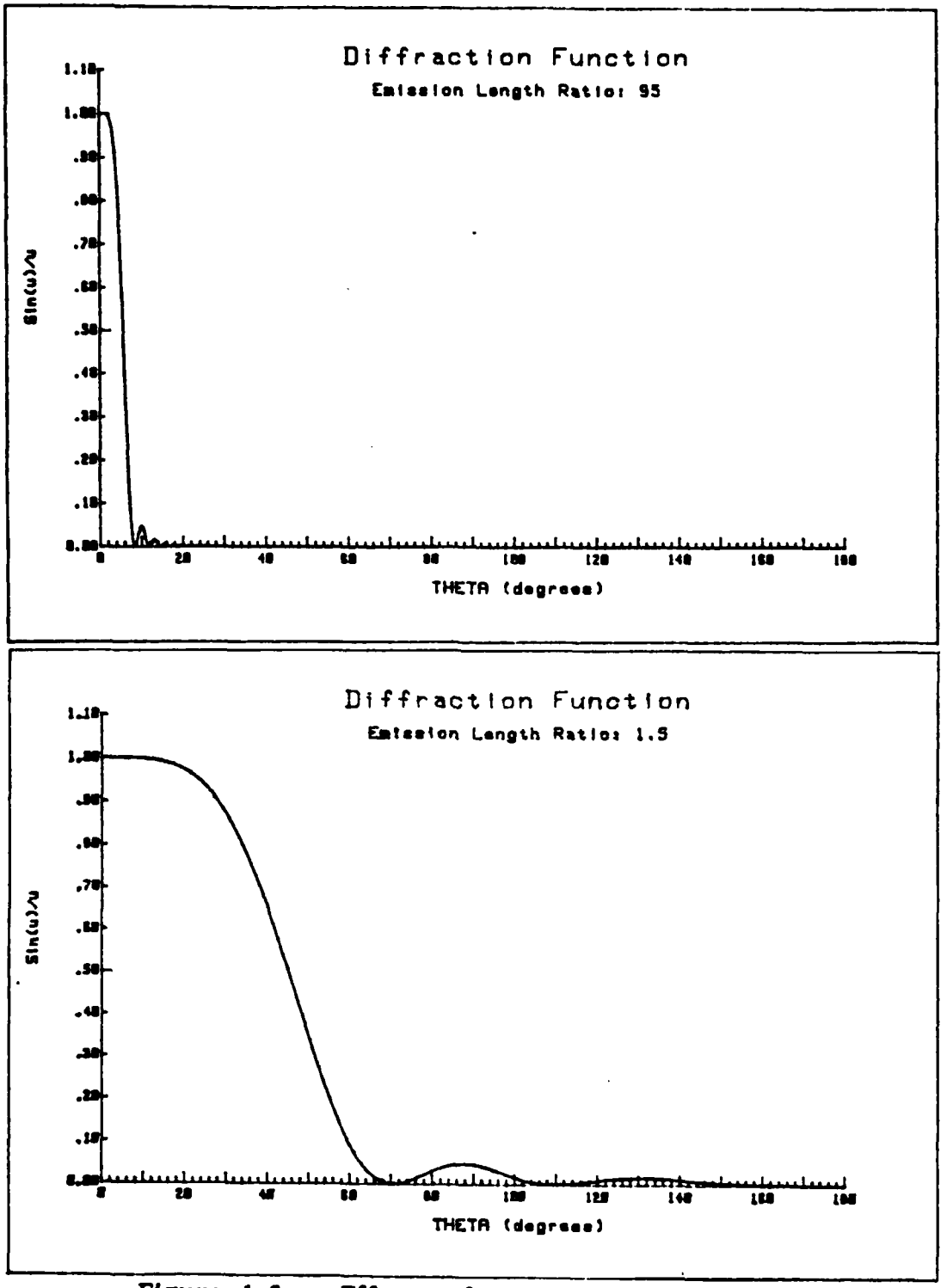

Figure 1.2 Effects of the Emission Length Ratio

reveals a characteristic ratio of lengths which has a profound effect on the resultant radiation pattern created by I(u). The emission length to wavelength ratio, L/λ, determines the periodicity of the diffraction pattern and also determines it's magnitude. Figure 1.2 shows the effects of two values of the emission length ratio.

It is interesting to note that there is a minimum limit to this ratio below which no diffraction occurs. This can be determined by using equation 1.4 and solving for the zeroes of the emission angle. This was done in [Ref. 3]. The equation for the emission angle for the first right hand zero in I(u), in terms of the emission length ratio, L/λ, is

$$\theta_o = \cos^{-1}(c/v - \lambda/L) \tag{1.12}$$

This is the emission threshold for Cerenkov radiation and equation 1.12 clearly shows the effect of a finite path length L. The quantity within the parentheses must stay within the bounds

$$-1 \leq (c/v - \lambda/L) \leq 1 \tag{1.13}$$

corresponding to the limits of $\theta = 180^\circ$ and $\theta = 0^\circ$. This condition provides the limiting case for the emission ratio where the angle is in the back direction. Then, using the left hand limit of equation 1.13,

$$L/\lambda = 1/(c/v + 1) \tag{1.14}$$

This gives a value of slightly greater than 1/2 for 100 MeV electrons in air. The requirement to have a phase relation of $\lambda/2$ generated from a minimum of two points within the emission path in order to have destructive interference dictates this limiting value. This condition becomes closely analogous to single slit diffraction only slightly modified by the Cerenkov condition. If we consider the threshold value of the electron velocity for which Cerenkov

A more specialized form of equation 1.2 can be obtained by introducing the harmonic number, j, which is related to the frequency by

$$j=\nu/\nu_o \tag{1.6}$$

Equation 1.2 now can be rewritten as

$$W_j(\theta)=QD_j(\theta) \tag{1.7}$$

The parameters are

$$Q=(\mu/2c)\nu_o^2q^2 \tag{1.8}$$

$$D_j(\theta)=j^2\nu_o^2L^2\sin^2\theta I^2(u)F^2(k) \tag{1.9}$$

where the product of the electron bunch charge, q, and the bunch form factor, F(k), has been substituted for the fourier transform of the charge density distribution, $\rho(k)$.

$$qF(K)\equiv\rho(k) \tag{1.10}$$

C. EFFECT OF THE FORM FACTOR

The focus of this paper is to investigate the behavior of the form factor and how it effects the radiated microwave power. To explain this effect, it is necessary to first consider the diffraction function, I(u). It will be this function that will determine the radiation pattern. Restating the diffraction variable in equation 1.3 in terms of the wavelength of the radiation in the medium as

$$u=\pi L/\lambda(c/v-\cos\theta) \tag{1.11}$$

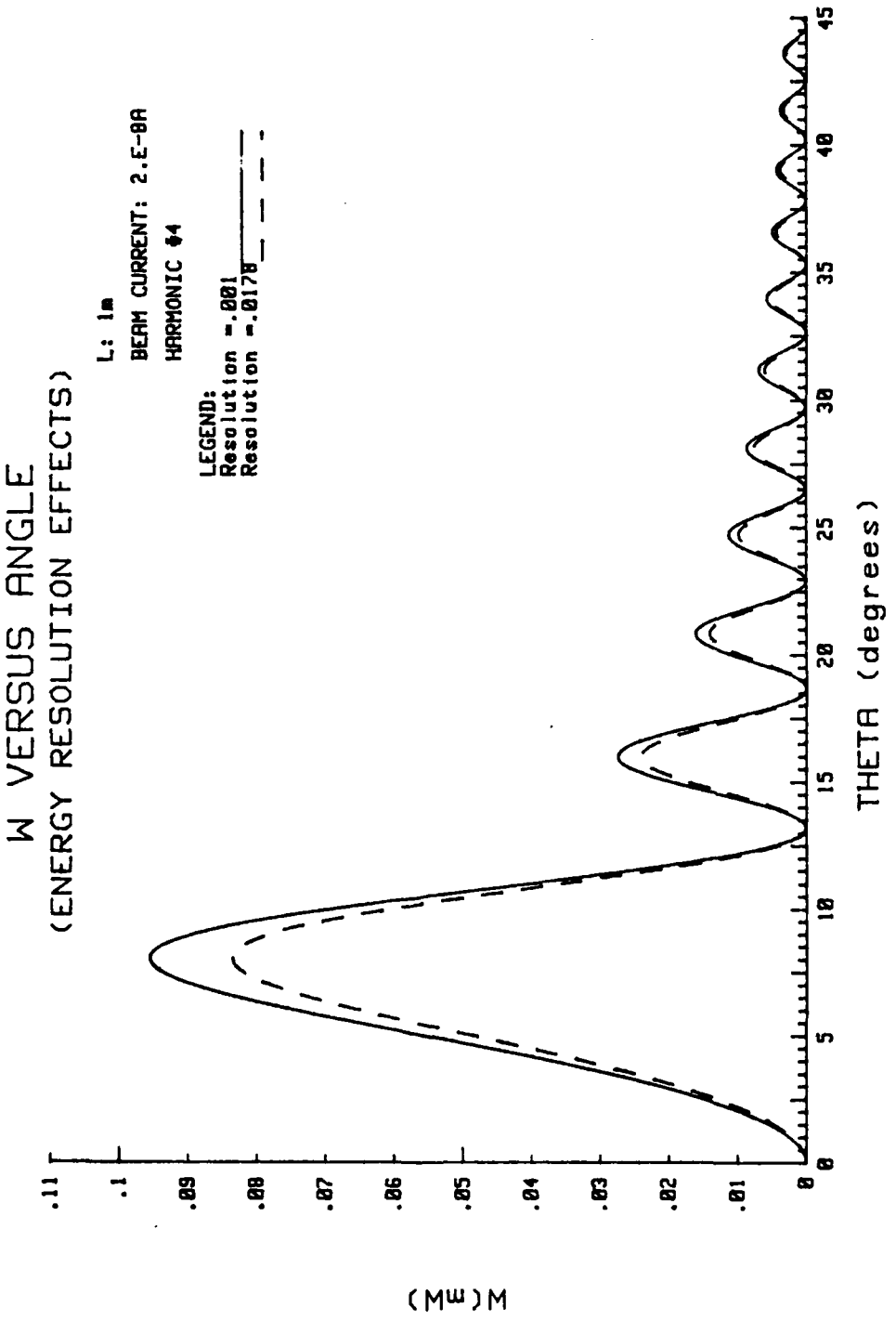

Figure 2.3 Radiated Power for the Fourth Harmonic

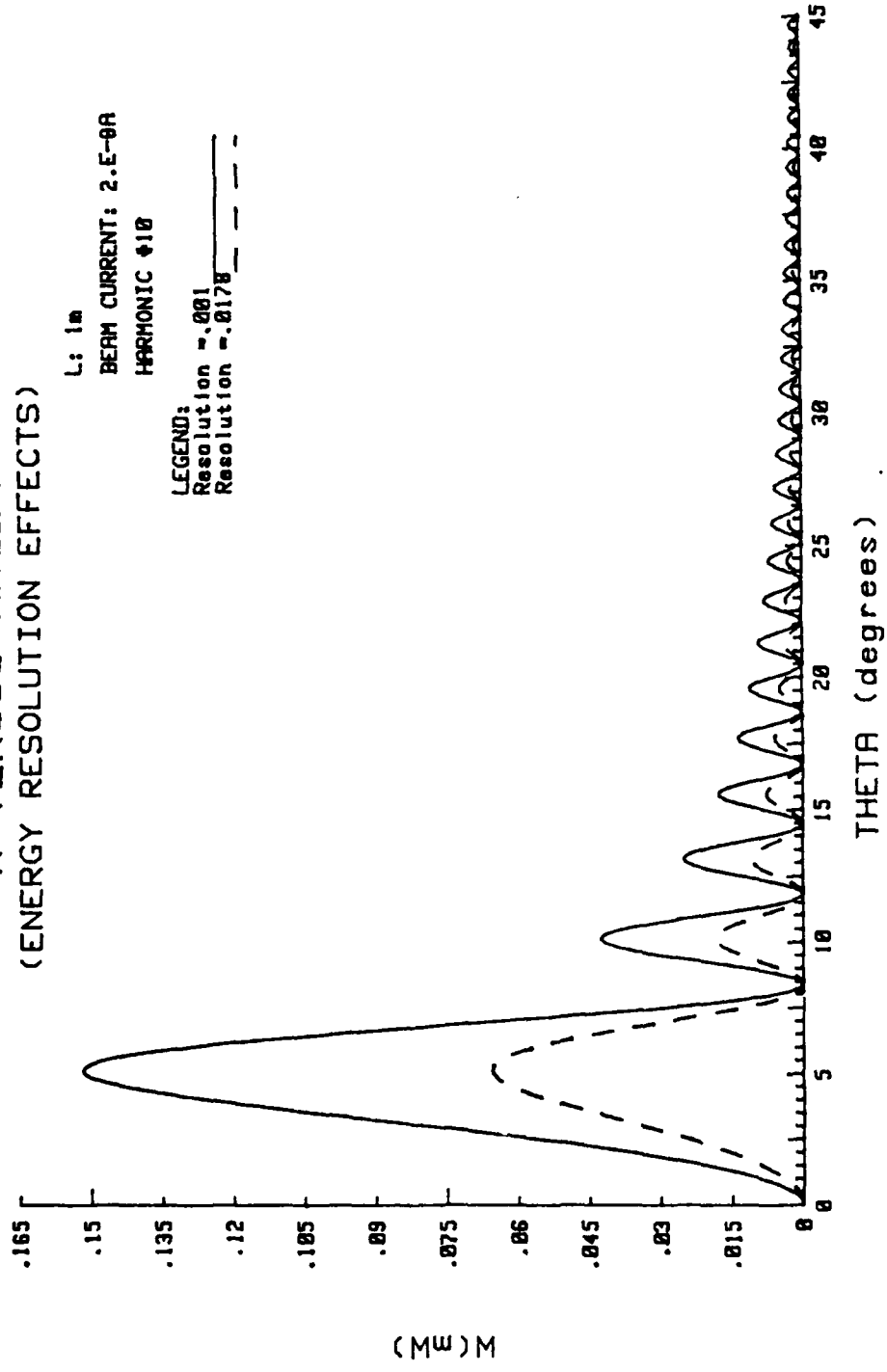

Figure 2.4 Radiated Power for the Tenth Harmonic

due to the bunch length should be more pronounced. Using the extreme limits of the bunch length available from the NPS LINAC results in about a ten percent change in power at the peak of the first lobe for the fourth harmonic. Whereas the tenth harmonic shows better than a fifty percent change in signal strength. Figure 2.5 displays the general result for all harmonics up to the twenty-fifth, and shows that the maximum radiation in the first peak depends strongly on the bunch size. Unfortunately, at the time of this experiment, an adequate amount of waveguide was only available for the X band. This limited the ability to detect only up to the fourth harmonic. The spectrum analyzer, therefore, had to be able to discern a ten percent change in signal strength for this data to be meaningful.

B. PROCEDURE

The procedure used in taking measurements was to establish an electron beam at constant current with the slit at its minimum separation. The peak was then located by moving the antenna until a maximum signal was realized. Once this position was located, the slit was opened slightly and current was reestablished. The value of the signal strength at each slit size was recorded. While conducting the experiment, it was realized that the ability of the LINAC to maintain a current which varied less than ten percent was barely within its capability.

A second method of detection was employed at this point. This method was based on improvements suggested by Newton in [Ref. 4]. For this method, the signal enters the antenna and is immediately amplified by a traveling wave tube (TWT) with an appropriate frequency band pass. The amplified signal is then filtered through a narrow band YIG filter which can be tuned from 1 to 18 GHz. The resultant signal is then converted to a voltage pulse by a crystal detector. From there, the pulse is transmitted through a triply shielded coaxial cable to an oscilloscope and a

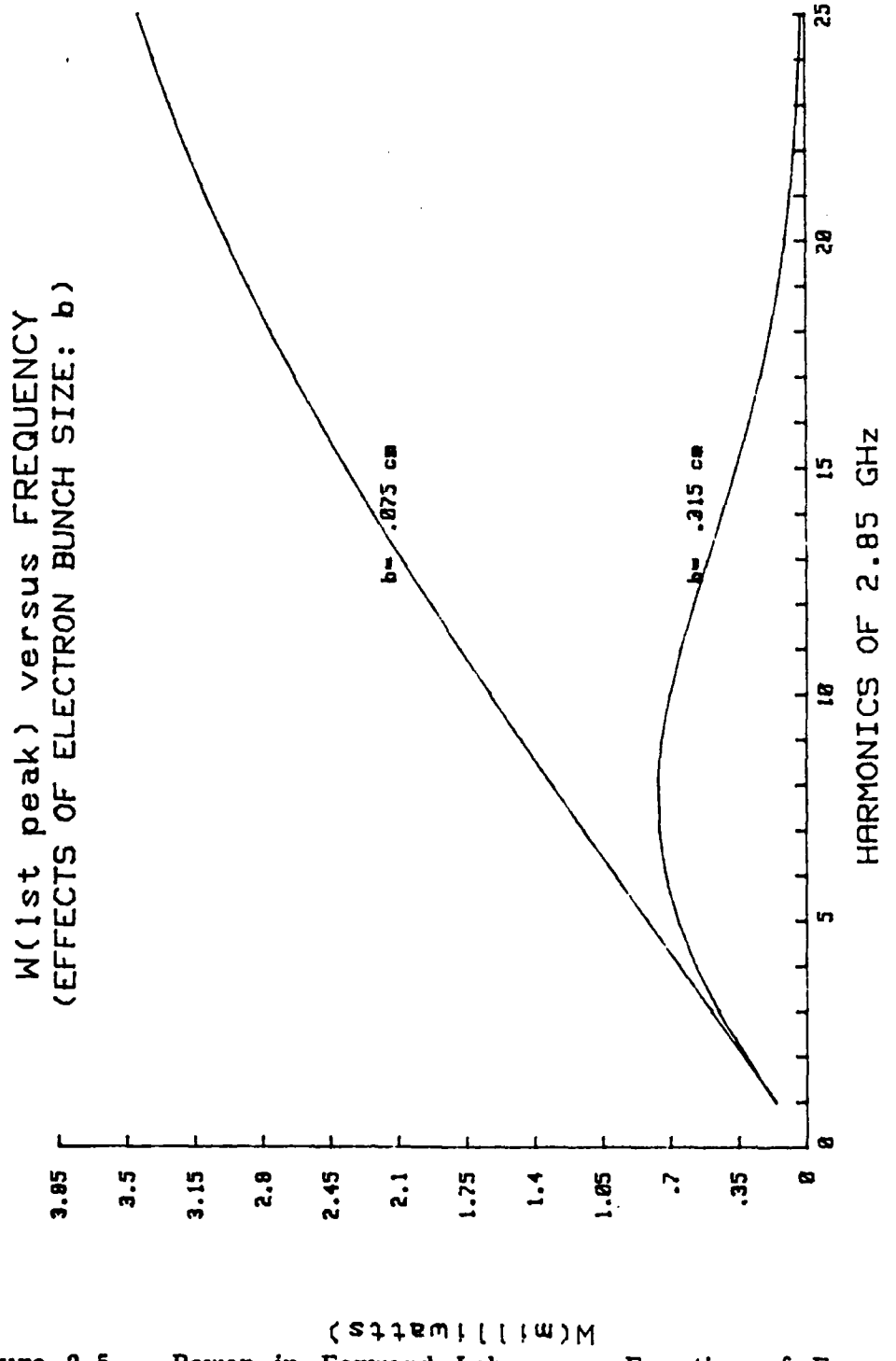

Figure 2.5 Power in Forward Lobe as a Function of Frequency

Tracor Northern Pulse Height Analyzer (PHA). Although the YIG filter was capable of detecting up to the sixth harmonic, it also provided a loss of about 20 decibels. TWT's were only available from 1 to 12 GHz which again meant detection only up to the fourth harmonic. At this point, the decision was made to continue collecting data on those harmonics available with the present equipment. A concerted effort by all concerned to attempt to reduce the fluctuations in the electron beam current would be necessary.

III. RESULTS AND CONCLUSIONS

A. RESULTS OF THE EXPERIMENT

The procedures described in Chapter 2 were conducted for the first through the fifth harmonics of the NPS LINAC's operating frequency. The results of this effort are displayed graphically in Figure 3.1 through Figure 3.5. For a given harmonic, the theoretical curve is obtained by plotting the value of power at the peak of the forward lobe as a function of the bunch length parameter, b. In doing this, the wave number k, the emission angle, θ, and the emission length L are kept constant. By normalizing the theoretical curve so that the value for b=0 is unity, the curve represents the square of the form factor. (see equation 1.9) The experimental points for each individual run are normalized to their mean value. A precision of fifteen percent was given to this data. The fluctuation in the electron beam current was considered to be the most significant contributor to this value.

As mentioned previously, attempts to improve the stability of the electron beam current were a major concern throughout the series of experiment. One of the actions taken in this regard was to attempt to insure that the LINAC was optimally tuned during the course of an experiment. This involved adjusting the power klystron timing and the phase relationship between the three waveguide sections within the LINAC.

It was discovered, however, that in the process of tuning during an experiment, the resulting pulse form and pulse magnitude of the microwave power could be changed without affecting the electron beam current. This indicated that there were parameters being affected by the tuning that were not being considered in the original procedure. It was decided to make some additional measurements in an attempt to determine the nature of this apparent discrepancy.

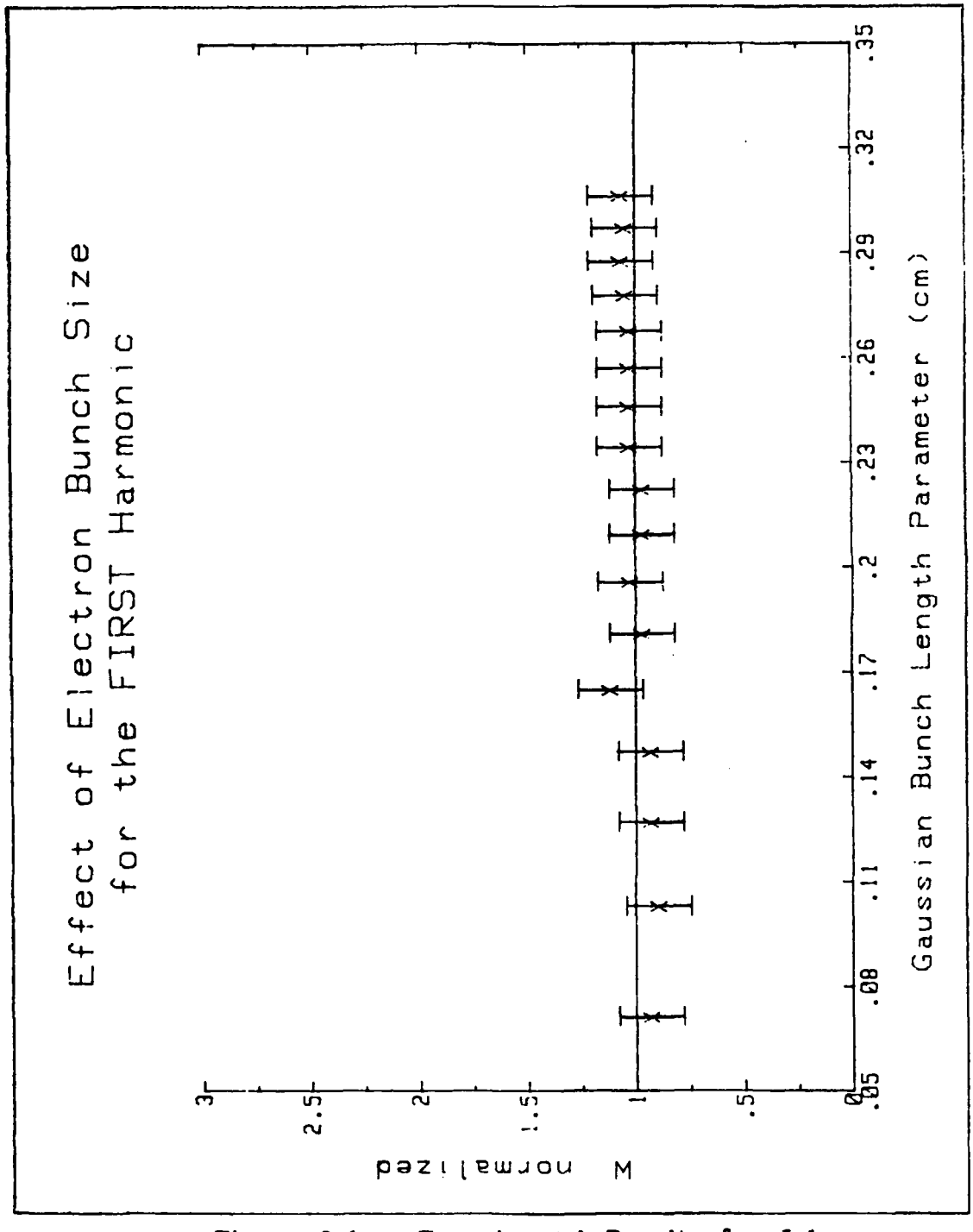

Figure 3.1 Experimental Results for J=1

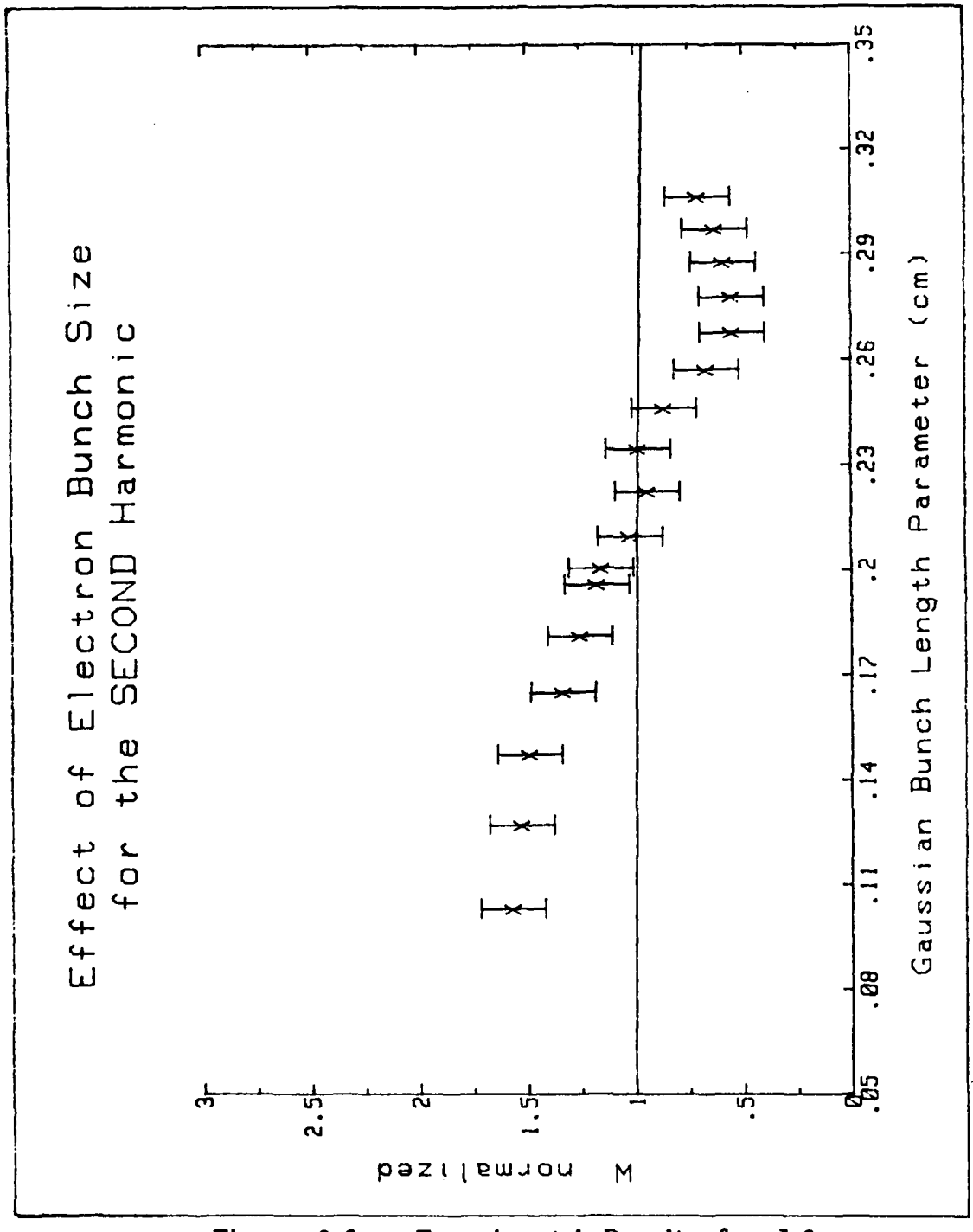

Figure 3.2 Experimental Results for J=2

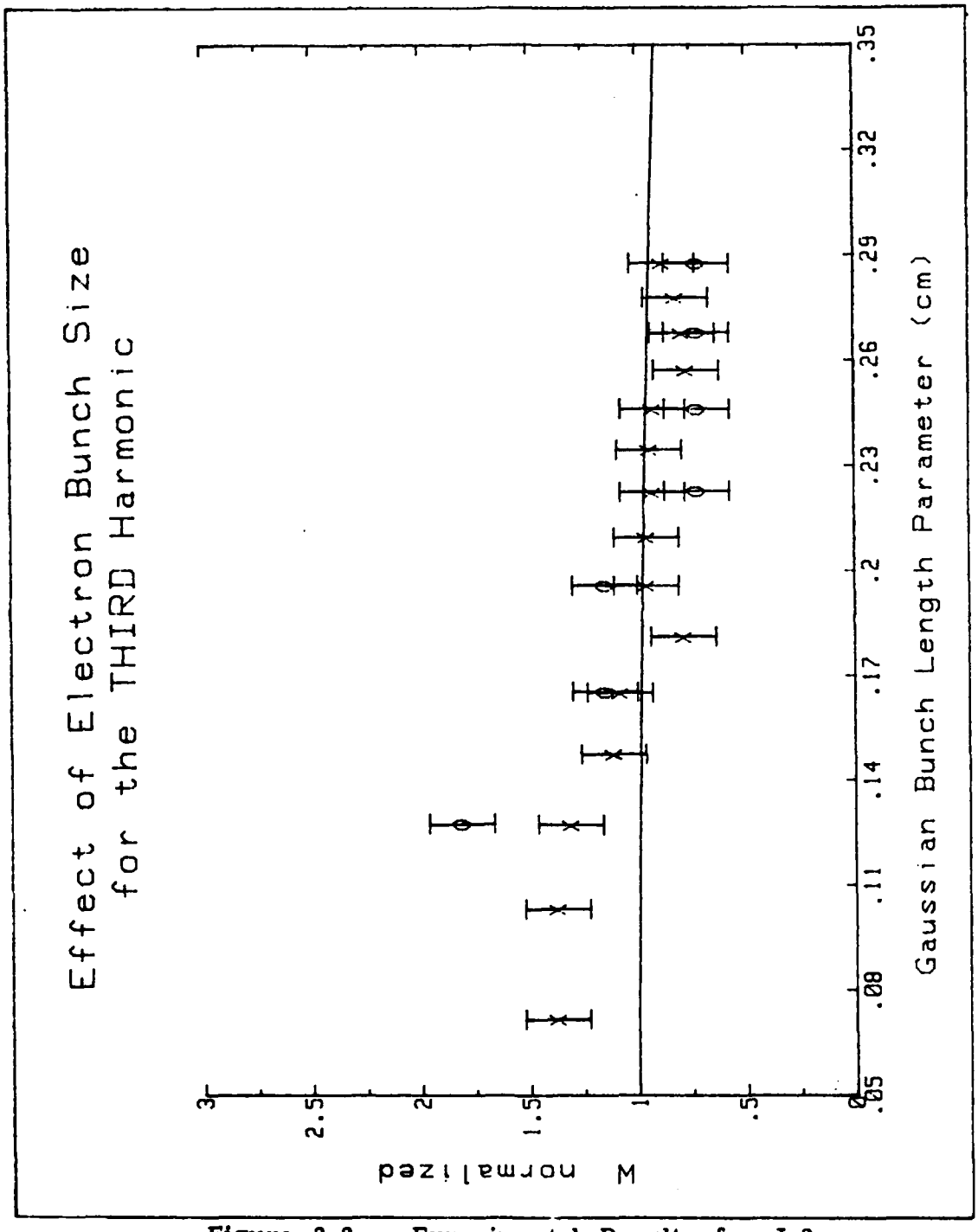

Figure 3.3 Experimental Results for J=3

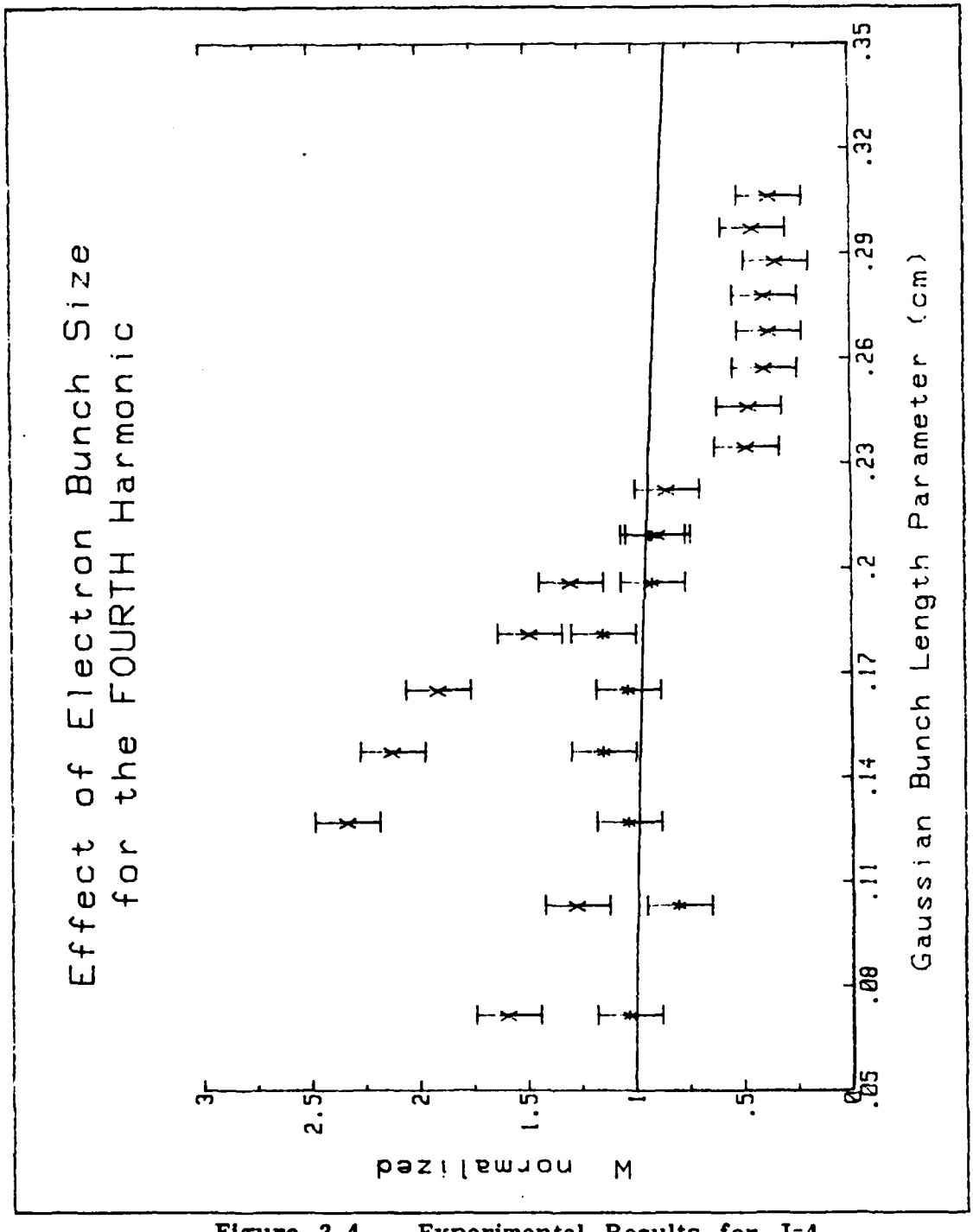

Figure 3.4 Experimental Results for J=4

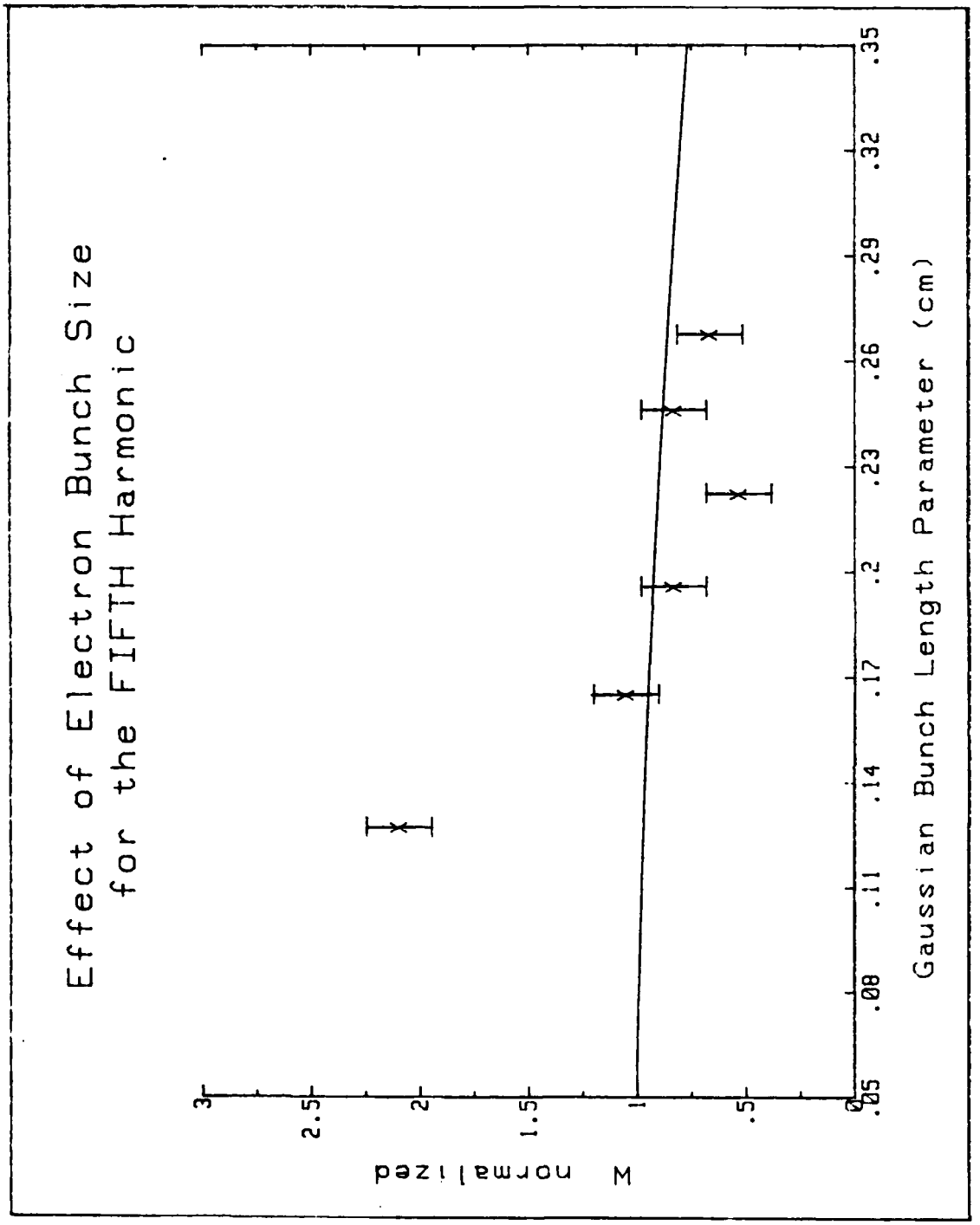

Figure 3.5 Experimental Results for J=5

One finding, as a result of this investigation, was that the inherent energy resolution of the LINAC can be substantially improved from the 1.36 percent originally determined. This can be readily seen in Figure 3.6 where two additional sets of data are superimposed over the preliminary data first presented in Figure 2.1. Although the two curves were taken on different occasions, which accounts for the shift in the maximum current available, they do indicate a shift in the upper current limit away from the original value of 350. This change in the inherent energy resolution is apparently dependent on the degree of tuning.

Another finding concerns the Cerenkov power dependence on the current. To determine this relation, measurements of the microwave power contained in the fourth harmonic were taken while keeping the slit size fixed and varying the beam current. For this experiment, the electron gun grid voltage was varied to cause a corresponding change in the beam current. The results are presented in Figure 3.7. An analysis of this data produces interesting results. Below an SEM current of about ten nanoamps (beam current below 0.17 microamps), the signal displays a second power dependence on the current as predicted by theory. However, for current above this value, the microwave power appears to follow the fourth power of current. The reason for this behavior is unknown.

B. CONCLUSIONS

The purpose of this series of experiment was to investigate the nature of the electron bunch charge distribution. The data presented in Figure 3.1 through Figure 3.5 are the products of this attempt. Only for the case of the first harmonic does the experimental measurements seem compatible with the theoretical predictions. For the other harmonics measured, a behavior other than that predicted occurs. The reasons for this apparent discrepancy are not entirely understood. While performing the experiment,

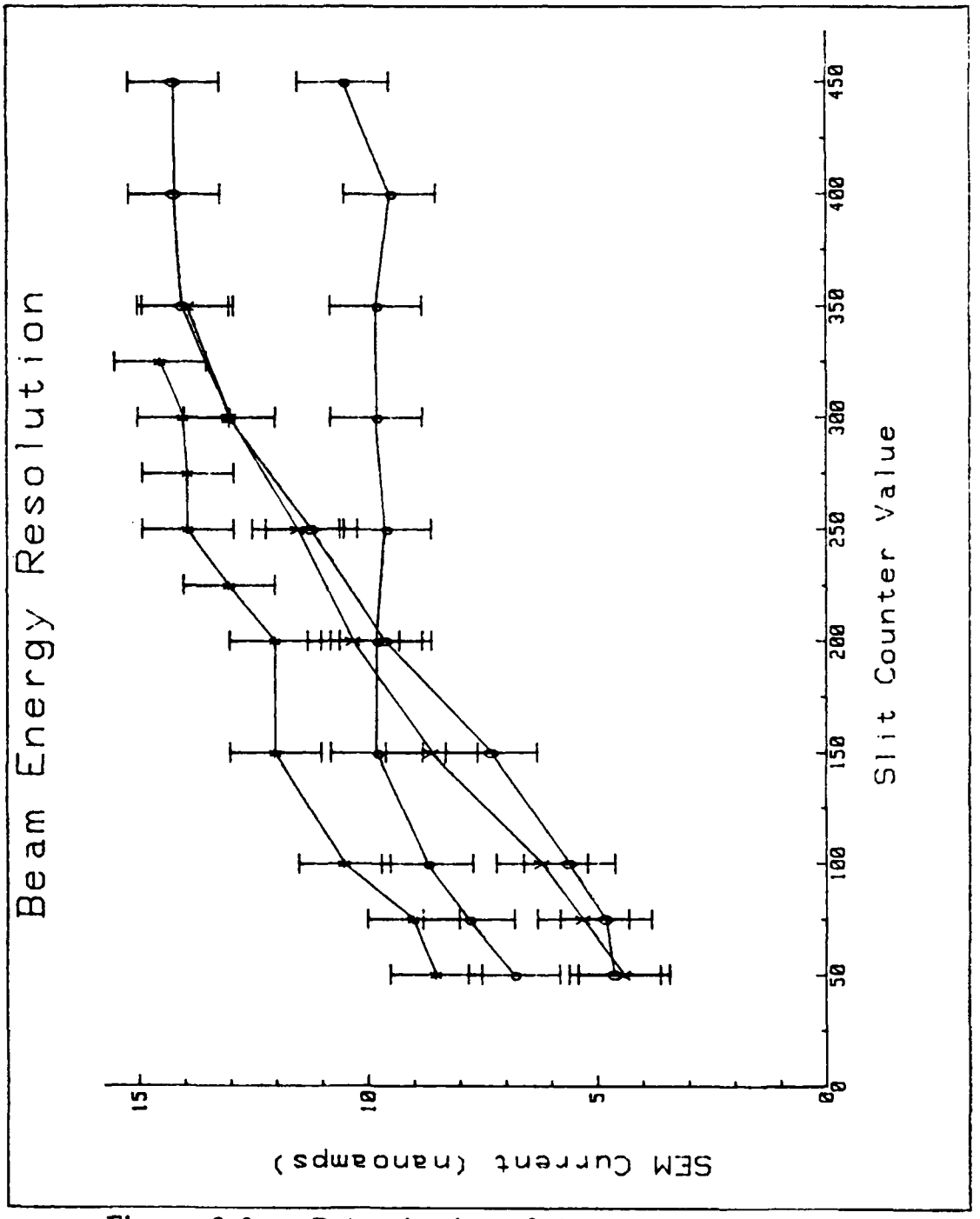

Figure 3.6 Determination of Inherent Bunch Length.

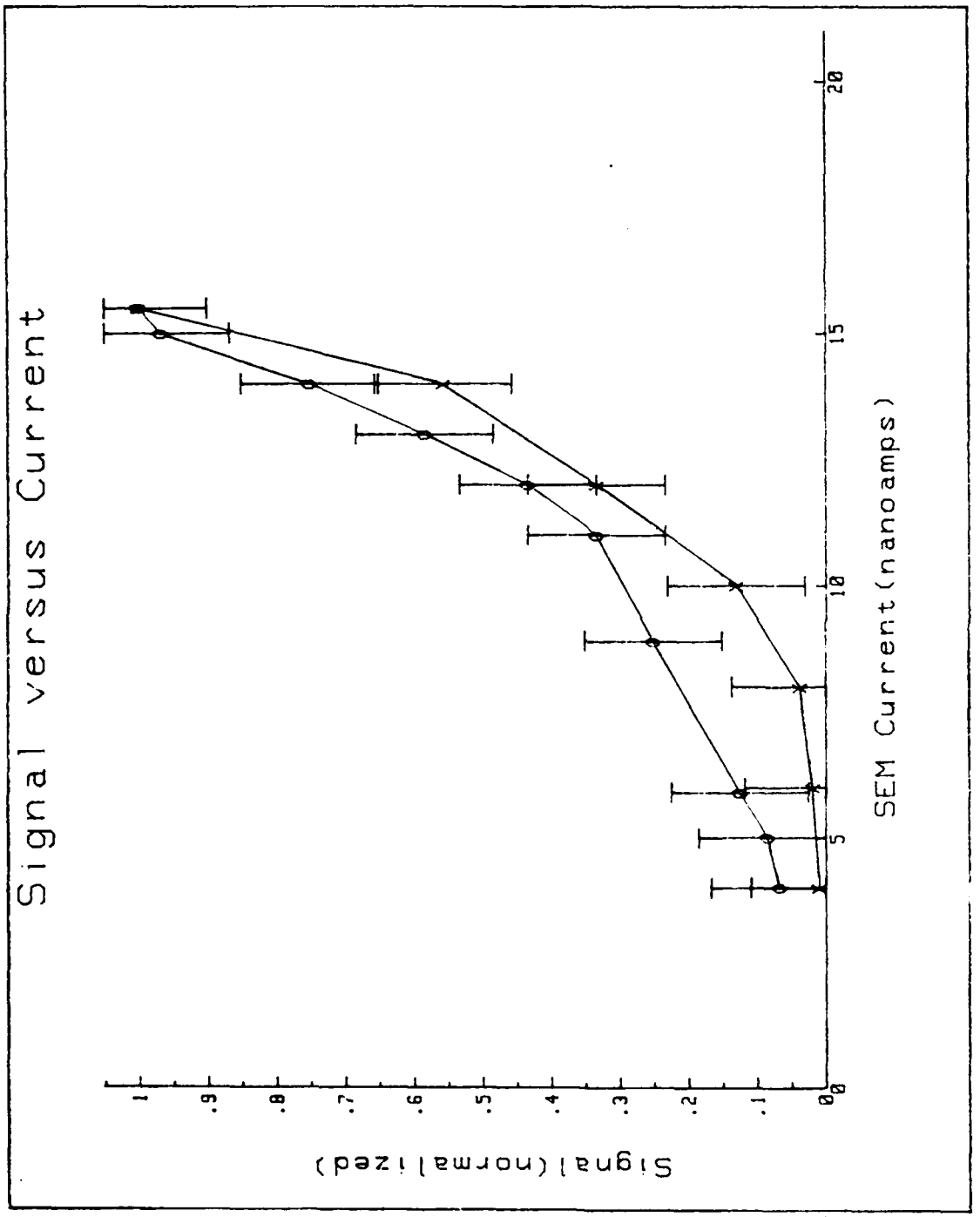

Figure 3.7 Determination of Current Dependence

new information was discovered which could account for a significant amount of this discrepancy. These discoveries impact on the experimental results in the following ways:

1. For the assumed range of bunch sizes available from the NPS LINAC, the largest expected change in signal strength would occur for measurements of the fifth harmonic and would be less than twenty percent. The majority of this difference is absorbed by the random errors of the system.

2. The discovery of the dependence of the maximum energy resolution value on tuning could have possibly caused the actual bunch size to be different than that which was assumed during the experiment. This can be better explained by using an example. Referring to Figure 3.6, if the LINAC were tuned to produce the data designated by the symbol "o" in Figure 3.6, any slit size value above the value of 100 on the horizontal scale would have no effect on the energy resolution hence no effect on the bunch size. If this fact were not known, the data would be erroneously recorded.

3. For beam current above 0.17 microamps, the signal's dependence on current appears to be greater than the second power. This was not predicted in the theory, and must be resolved before any qualitative statement can be made about the form factor.

C. SUGGESTIONS FOR FUTURE STUDY

Improvements in both equipment and procedures must be made for any further study into the nature of the electron bunch charge distribution using the NPS LINAC. The knowledge gained during this attempt can be summarized into the following suggestions.

Any meaningful effort will require the measurement of higher order harmonics. Obtaining the equipment necessary to accomplish this should receive high priority. As discussed in Chapter 2, there are at least two detector configurations which will accomplish

this. Equipment deficiencies were identified to exist for both methods. Either method could be used successfully.

In order to insure that the bunch length is being affected by the energy defining system, I recommend that once the LINAC is tuned a series of measurements be made of the current as a function of slit opening. This will determine the inherent maximum bunch length being produced by the accelerator and will become the maximum limit for that run. At this point an attempt could be made to retune the LINAC in order to produce a larger bunch. Caution is recommended here since the current stability and maximum available current could be adversely affected. Once this maximum has been established, neither the timing nor the phase of the machine should be changed until the experiment is completed. The requirement for a constant current can be maintained by adjustment of the frequency and the electron gun grid voltage only. This procedure should be repeated every time the timing or the phase of the LINAC is changed.

A consequence of the k_z dependence of the form factor is the the predicted radiation at an angle normal to the electron beam path in the emission region. This is discussed in Chapter 1. Detection and subsequent measurement of this radiation could lead to a better understanding of the electron charge distribution. Efforts to configure the target area in order to measure this radiation should be pursued.

A related topic of interest which warrants further investigation is the microwave power dependence on current. Inherent to the study of Cerenkov microwave radiation is the theoretical second power dependence on current. The present finding implies a deviation from this. It may be, perhaps, that some component of the system which has not been accounted for is providing this indication. In any case, verification of this dependence is highly recommended.

APPENDIX A
DERIVATION OF THE ELECTRON BUNCH PARAMETER

The electron bunches produced by a traveling wave accelerator contain a finite spectrum of energies due to the energy exchange mechanism. In order to have some control over the extent of this spectrum, the NPS LINAC incorporates a deflection system consisting of a bending magnet and an energy defining slit. As the electrons in the bunch pass through the bending magnet, they are deflected with a radius proportional to their energies. The electrons then encounter the narrow slit which is positioned to pass only those electrons traveling within a defined range of trajectories. This allows the production of a highly monoenergetic electron beam. The slit opening can be adjusted to vary the degree of this energy spectrum.

Using a development similar to that contained in [Ref. 6], assume the energy of an individual electron as it enters the deflection system with a phase ϕ relative to the traveling wave is

$$E=E_{\circ}\cos\phi \tag{A.1}$$

where E is the central energy. If the deflection system passes only energies E from $E_{\circ}$ to $E_{\circ}\pm\Delta E$, then the least energetic electron to pass would have an energy

$$E_{\circ}-\Delta E=E_{\circ}\cos\phi \tag{A.2}$$

If ϕ is small, this reduces to

$$\Delta E/E_{\circ}=\phi^2/2 \tag{A.3}$$

ϕ becomes the acceptance angle and is related to the LINAC operating frequency, ν_o, and the bunch length, b, by the relation

$$\phi/(2\pi)=b\nu_o/v \qquad (A.4)$$

or, in terms of the LINAC energy resolution, $\Delta E/E$,

$$b=[2\Delta E/E]^{1/2}v(2\pi\nu_o)^{-1} \qquad (A.5)$$

The distance between pulses, d, becomes

$$d=\ell-b=v\nu^{-1}[1-(2\Delta E/E)^{1/2}(2\pi)^{-1}] \qquad (A.6)$$

For an operating frequency of 2.856 GHz and an energy resolution of one percent, equation A.5 produces a bunch length of 0.236 centimeters. The distance between pulses is calculated by equation A.6 to be 10.3 centimeters.

APPENDIX B
METHOD TO EXPERIMENTALLY DETERMINE F(K)

Starting with the equations developed in Chapter 1, the power per unit solid angle can be expressed as

$$W=Q(L/\lambda)^2\sin^2\theta F^2(k_z)\sin^2(u)/u^2 \qquad (B.1)$$

This can be rearranged as

$$Wu^2/(Q^2\sin^2\theta)(\lambda/L)^2=\sin^2\theta F^2(k_z) \qquad (B.2)$$

All quantities in the left side are either known or experimentally obtainable. Namely, these are: the beam current, the length of the emission region, the frequency being observed, and the emission angle θ, measured from the center of the emission region L/2. If the values of W are measured while varying only the emission angle, then a plot of the left side of equation B.2 will produce a rapidly oscillating sine function of u whose envelope will represent the form factor, $F(k_z)$. This envelope can then be transformed to obtain the one dimensional electron density distribution, $\rho(z)$. This method can thus be used to determine the actual bunch structure. The experimental procedures necessary to accomplish this task are not realizable with the current equipment and physical constraints at the NPS LINAC and should be considered a subject for future research.

APPENDIX C
TABULATION OF DATA

The following tables of data were used to develop the plots presented in Chapters 2 and 3. The corresponding figure for each table is provided.

TABLE 2
Signal Dependence on Current

Plotted in Figure 3.7

SEM Current(na)	Signal(mV) Plotted as: "X"	"O"
15.5	5.4	0.60
15.0		0.58
14.0	3.0	0.45
13.0		0.35
12.0	1.8	0.26
11.0		0.20
10.0	0.8	
0.89		0.15
0.80	0.2	
0.60	0.1	
0.59		0.075
0.50		0.051
0.40	0.05	0.040

For Table 3 through Table 7, the values of signal strength listed in units of watts were obtained using the Tektronix 7L18 spectrum analyzer. All other values were obtained using the YIG filter-oscilloscope configuration described in Chapter 2. The equations that relate the slit counter value to the electron bunch size are also provided in Chapter 2.

TABLE 3

Bunch Size Effects for the First Harmonic

Plotted in Figure 3.1

Slit Counter Value	Signal (mv)
50.2	2.50
75.0	2.40
100.0	2.50
125.0	2.50
150.0	3.00
175.0	2.60
200.0	2.75
225.0	2.60
250.0	2.60
275.0	2.75
300.0	2.75
325.0	2.75
350.0	2.75
375.0	2.80
400.0	2.85
425.0	2.80
450.0	2.85

TABLE 4

Bunch Size Effect for the Second Harmonic

Plotted in Figure 3.2

Slit Counter Value	Signal (mV)
50.0	0.49
75.0	0.40
100.0	0.39
125.0	0.38
150.0	0.34
175.0	0.32
200.0	0.30
225.0	0.26
250.0	0.24
275.0	0.25
300.0	0.22
325.0	0.17
350.0	0.14
375.0	0.14
400.0	0.15
425.0	0.16
450.0	0.18

TABLE 5

Bunch Size Effect for the Third Harmonic

Plotted in Figure 3.3

Slit Counter Value	Signal (cm) Plotted as: "X"(mv)	"O"(μw)
50.0	0.78	2.51
75.0	0.70	
100.0	0.67	
125.0	0.60	
150.0	0.57	1.59
175.0	0.51	
200.0	0.62	1.59
225.0	0.62	
250.0	0.60	1.00
275.0	0.61	
300.0	0.60	1.00
325.0	0.50	
350.0	0.51	1.00
375.0	0.53	
400.0	0.57	1.00

TABLE 6

Bunch Size Effect for the Fourth Harmonic

Plotted in Figure 3.4

Slit Counter Value	Signal(mV) Plotted as: "X"	"*"
50.0	0.35	0.09
75.0	0.42	0.07
100.0	0.32	0.09
125.0	0.37	0.10
150.0	0.35	0.09
175.0	0.37	0.10
200.0	0.44	0.08
225.0	0.45	0.08
250.0		0.80
275.0		0.84
300.0		1.22
325.0		1.40
350.0		1.80
375.0		2.00
400.0		2.20
425.0		1.20
450.0		1.50

TABLE 7

Bunch Size Effect for the Fifth Harmonic

Plotted in Figure 3.5

Slit Counter Value	Signal (μw)
100.0	0.63
150.0	0.32
200.0	0.25
250.0	0.16
300.0	0.25
350.0	0.20

TABLE 8

Slit Size Effects on Beam Current

Plotted in Figure 3.6

Slit Counter Value	SEM Current (nanoamps) Plotted as: "X"	"O"	"o"	"*"
50.0	4.4	4.6	6.8	8.5
75.0	5.3	4.8	7.8	9.0
100.0	6.2	5.6	8.7	10.5
125.0				9.7
150.0	8.9	7.3	9.8	12.0
175.0				9.8
200.0	10.6	9.6	9.8	12.0
225.0			9.8	13.0
250.0	11.5	11.2	9.6	13.9
275.0				13.9
300.0	13.0	13.0	9.8	14.0
323.1				14.5
350.0		13.9	14.0	9.8
400.0			14.2	9.5
450.0			14.2	12.5

LIST OF REFERENCES

1. Naval Postgraduate School, Report Number NPS-61-83-003, *Cerenkov Radiation from Bunched Electron Beams*, by F.R. Buskirk and J.R. Neighbours, October 1982.

2. Naval Postgraduate School, Report Number NPS-61-83-010, *Diffraction Effects in Cerenkov Radiation*, by John R. Neighbours and Fred R. Buskirk, June 1983.

3. Naval Postgraduate School, Report Number NPS-61-84-010, *Radiation from Intense Electron Beams Associated with the Cerenkov Mechanism*, by J.R. Neighbours and F.R. Buskirk, June 1984.

4. Newton, Lawrence A., *Cerenkov Radiation Generated by Periodic Electron Bunches in a Finite Air Path*, Master's Thesis, Naval Postgraduate School, Monterey, 1983.

5. Pugh, Kenneth S., *Stimulated Cerenkov Radiation Beam Monitor*, Master's Thesis, Naval Postgraduate School, Monterey, 1983.

6. Saglam, Ahmet, *Cerenkov Radiation*, Master's Thesis, Naval Postgraduate School, Monterey, 1982.

INITIAL DISTRIBUTION LIST

		No. Copies
1.	Defense Technical Information Center Cameron Station Alexandria, Virginia 22314	2
2.	Superintendent Attn: Library, Code 0142 Naval Postgraduate School Monterey, California 93943	2
3.	Physics Library, Code 61 Department of Physics Naval Postgraduate School Monterey, California 93943	1
4.	Professor J. R. Neighbours, Code 61Nb Department of Physics Naval Postgraduate School Monterey, California 93943	5
5.	Professor X. K. Maruyama Code 61Xa Department of Physics Naval Postgraduate School Monterey, California 93943	5
6.	Professor F. R. Buskirk Mail Stop P940 Los Alamos National Laboratory Los Alamos, New Mexico 87545	1
7.	Mrs. E. P. Turner 151 North Spring Road Vineland, New Jersey 08360	3
8.	Lcdr. E. R. Turner 3220 Kinross Circle Herndon, Virginia 22071	2

END

FILMED

7-85

DTIC